Available online at www.sciencedirect.com
SCIENCE DIRECT®
International Journal of Heat and Mass Transfer 48 (2005) 527–535
International Journal of HEAT and MASS TRANSFER
www.elsevier.com/locate/ijhmt

Heat sink applications of extruded metal honeycombs

B.M. Dempsey, S. Eisele, D.L. McDowell *

The George W. Woodruff School of Mechanical Engineering, Georgia Institute of Technology, Atlanta, GA 30332-0405, USA

Received 16 January 2004; received in revised form 10 September 2004
Available online 6 November 2004

Abstract

Linear Cellular Alloys (LCAs) are metal honeycombs that are extruded using powder metal-oxide precursors and chemical reactions to obtain near fully dense metallic cell walls. Either ordered periodic or graded cell structures can be formed. In this work, the performance of heat sinks fabricated from stochastic cellular metals is compared to that of LCA heat sinks. Flash diffusivity experiments are performed to determine the in situ thermal properties of cell wall material. The pressure drop for unidirectional fluid flow in the honeycomb channels and the total heat transfer rate of LCA heat sinks are experimentally measured. These measurements are compared to values predicted from a finite difference code and commercial computational fluid dynamics (CFD) software.

Keywords: Heat transfer; Cellular materials; Conductivity; Pressure drop

1. Introduction

Cellular metals are low density materials that combine certain stiffness, strength, crushing energy absorption and thermal characteristics, such as high surface area to volume ratios and high conductivity walls, in a way that makes them attractive for use in heat sinks. Cellular metals are composed of cells that can be categorized as (i) either open or closed foams and (ii) either stochastic or ordered. Regardless of the classification, cellular metals have a relative density given by ρ/ρ_s [1], where ρ is the density of the cellular metal and ρ_s is the density of the solid cell wall material. Various cellular material properties such as elastic stiffness, effective thermal conductivity, and effective yield strength can be directly related to the properties of the solid comprising the cell walls through the relative density [2]. Traditional polymeric and ceramic foams are known for their ability to insulate and inhibit the transfer of heat, e.g. polystyrene [1], quite distinct from heat exchange goals with cellular metals.

1.1. Stochastic cellular materials

Stochastic cellular metals can be made using several techniques [2], ranging from stirring foaming agents into molten metal to making an organic mold that is filled with molten metal or powder metal slurries and then the organics are burned out. The resulting cellular structure looks very much like cell structures in natural organic materials, as shown in Fig. 1.

When used as a heat sink, stochastic open-cell cellular metals are a porous medium through which coolant flows. High conductivity cell walls or edges facilitate heat flow from the source into the sink. A common heat

* Corresponding author. Tel.: +1 404 894 5128; fax: +1 404 894 0186.
E-mail address: david.mcdowell@me.gatech.edu (D.L. McDowell).

0017-9310/$ - see front matter © 2004 Elsevier Ltd. All rights reserved.
doi:10.1016/j.ijheatmasstransfer.2004.09.013

Nomenclature

A_c	cross-sectional area
c_p	specific heat
D_h	hydraulic diameter
d	internal diameter of square cell
f	friction coefficient
g	gravitational constant
h_L	head loss
K	loss coefficient
k	thermal conductivity
L	heat sink length
L_α	thickness of diffusivity specimen
$\dot{m}$	mass flow rate
n	counter variable
P	pressure
P_w	wetted perimeter
ΔP	change in pressure from inlet to exit of heat sink
$\dot{Q}$	heat transfer rate
Re	Reynolds number
T	temperature
T^*	normalized temperature
ΔT	change in temperature
t	cell wall thickness
$\bar{v}$	mean velocity
z	height

Greek symbols

α	thermal diffusivity
γ	specific weight
μ	dynamic viscosity
ρ	density
T	time
ω	normalized diffusivity

Subscripts

E	expansion
f	fluid
I	inlet contraction
s	solid

sink arrangement for unidirectional flow is shown in Fig. 2.

In this configuration, heat is transferred via forced convection to the coolant, which flows in the positive z-direction in Fig. 2. Advantages of this porous structure include high surface area to volume ratio, as well as the enhancement of the heat transfer coefficient associated with turbulent patterns formed in the coolant [1]. The disadvantage of these stochastic porous structures is the large pressure drop in the fluid that requires increased pump power to drive the coolant flow [1,3]. This is primarily due to stagnation flow at the projections of the cell wall segments normal to the nominal flow velocity.

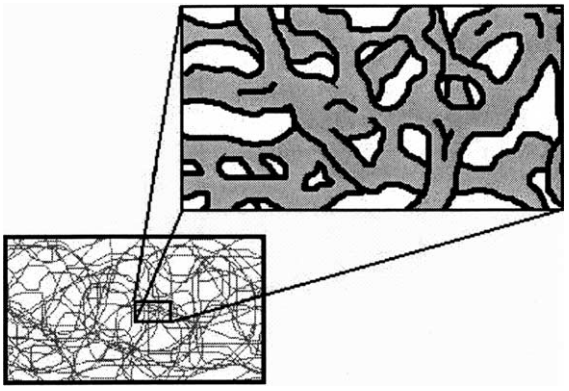

Fig. 1. Structure of stochastic open-cell cellular metal.

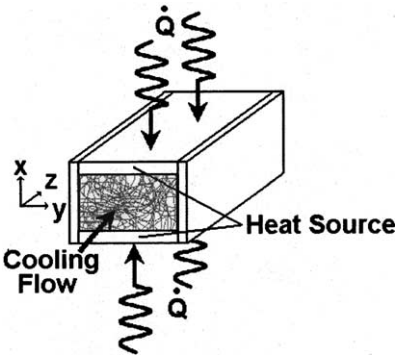

Fig. 2. Schematic of a stochastic cellular metal heat sink used to cool computer chips.

This setup was examined experimentally and numerically in Refs. [1,4]. Experiments were performed on aluminum cellular metal arranged in a manner similar to that shown in Fig. 2. The numerical simulations employed an approximation of the foam geometry as comprised of simple cubic unit cells consisting of banks of cylinders in various orientations.

1.2. Ordered cellular materials

Recent advances in low-cost manufacturing of ordered cellular metals have made it feasible to use these

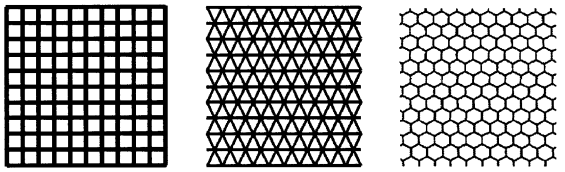

Fig. 3. Schematic cross sections of several honeycomb cross sections, including: (a) square cell, (b) triangular cell, and (c) regular hexagonal cell.

materials in heat transfer applications [2,5]. Common periodic cell structures of metal honeycombs are shown in Fig. 3. The heat transfer performance of a repeating hexagonal cell structure has been analytically modeled and compared to the performance of stochastic cellular metals by Lu [5]. Periodic square, triangular, and regular hexagonal cell structures have also been examined [6]. In most fan-driven, air-cooled heat sink applications, ordered cellular materials have a dominantly laminar flow and a low pressure drop, with a limited heat transfer coefficient. In contrast, stochastic foams generate turbulence that increases the local heat transfer coefficient [5], but develop substantially higher pressure drop. Of course, it is possible to operate in the turbulent regime via high speed flow through honeycombs as well, also resulting in increased pressure drop per unit length.

1.3. Applications

A procedure for processing metal honeycombs with a wide range of cell topologies has been developed within the Lightweight Structures Group at Georgia Tech [7] using metal-oxide powders, organic binders, and water to create a paste that can be extruded to form a two-dimensional cell structure in the green state, and then reduced in hydrogen to create the final prismatic metal honeycomb structure. This process is known as the Direct Reduction Method (DRM) and the resulting metallic cellular extrudate or honeycomb is referred to as a Linear Cellular Alloy (LCA).

Due to their high surface area to volume ratio, low pressure drop per unit length, and high cell wall conductivity, LCAs may provide a cost effective, compact solution to the needs of forced flow convective heat sinks. When fabricating very complex, fine-scale cell morphologies, the powder process used to produce the LCAs is more robust than sheet metal folding or welding processes used for conventional metal honeycombs. Although this work does not discuss the structural properties of LCAs, they exhibit high strength at low density [2,8], and therefore are candidates for multifunctional applications requiring strength, stiffness and thermal/heat transfer capabilities.

2. Experiments and comparisons for DRM LCA heat sinks

2.1. Flash diffusivity

The process used to create these LCAs leads to residual porosity of several percent in the cell walls and may also introduce residual oxide particles. The resulting in situ cell wall material has unknown thermal conductivity and diffusivity that differ from bulk metal of the same composition. To determine these properties, pellets were made for xenon flash diffusivity measurements. The measurements were performed within the High Temperature Materials Research Laboratory at Oak Ridge National Laboratory. Pellet specimens composed of pure Cu, Cu–3%Ni solid solution alloy, Cu–l%Ni, Cu–8%Ag, and Cu–l%Ag were examined. However, only the pure Cu was required for the experiments reported in this work. The pellet samples were made with a uniform thickness, L_α, for a one-dimensional xenon flash diffusivity experiment. In the experiment, a uniform xenon pulse of radiant energy is imposed on the front surface of the sample. The heat is transferred unidirectionally from the front surface to the back surface. The back surface temperature is monitored by an infrared camera. The thermal diffusivity was obtained by using the Parker Flash Method [9]. The method assumes that the material is isotropic and homogeneous, and is subjected to an instantaneous, uniformly distributed flash pulse on the front surface. The experimental setup records the time and corresponding back surface temperature. The non-dimensional temperature solution can be calculated with the formula [10]

$$T^* = 1 + 2\sum_{n=1}^{\infty}(-1)^n \exp(-n^2\omega^2) \tag{1}$$

where T^* is the normalized temperature, $T(L_\alpha,\tau)/T(L_\alpha,\tau)_{\max}$, τ is time, and $\omega = \pi^2\alpha\tau/L_\alpha^2$. Note that ω is related to the Fourier number by π^2. Using these data, the thermal diffusivity, α, is determined. By assuming an approximate value for the specific heat in conjunction with the measured values of thermal diffusivity and density, the thermal conductivity can be found via [11]

$$k = \alpha\rho_s c_p \tag{2}$$

where c_p is the specific heat of the solid. For comparison to known thermal conductivities, tabulated approximations of the specific heat were used to estimate the thermal conductivity of the samples [11,12]. When reduced at 1323 K, the thermal conductivity of the pure copper pellet was found to be 362.7 W/m K. It is noted that the thermal conductivity of pure Cu is approximately 400 W/m K. The thermal conductivity of the reduced and sintered porous cell wall materials considered in this paper lies within expected ranges [13,14].

2.2. Heat sink experiments

Heat sink experiments on a square cell honeycomb conform to the schematic shown in Fig. 4, with three sides insulated and the top or bottom surface subjected to prescribed temperature or heat flux. Fig. 5 provides a more detailed cross sectional view of the experimental set-up, with air flow from left to right. A 0–0.01 m^3/s flow meter is used to measure the flow rate of the air at the inlet. From this point, the air is forced through a large diffuser with a stochastic aluminum foam insert with cell size on the order of that of the LCA cell diameter to promote a more uniform flow distribution for air entering into the test section. The pipes that join the specimen to diffusers on each end have tapped holes that are used to determine the pressure drop of flow along the length of the LCA using a wet/wet low differential pressure transducer. The LCA is fixed at both ends into gaskets that are placed inside of the inlet and exit pipes. Teflon-coated T-type duplex insulated 30 AWG thermocouple wires are placed at various locations within the experimental setup to measure temperature profiles of the specimen and air temperatures. Compressed air as coolant is introduced through a standard 0.79 cm (5/16 in.) hose.

The output of thermocouples on the heat spreader and at the inlet and exit of the flow to the LCA specimen are used to control the heater power supply. The heat spreader is made of 6.4 mm thick high conductivity Cu plate to promote a more uniform temperature distribution over the region of contact with the LCA. A silicon rubber heater is attached to the heat spreader and is powered by a power controller. A PID temperature controller controls the power supply based on heater temperature as measured with a K-type thermocouple. A high temperature glass-coated K-type duplex insulated 24 AWG thermocouple wire is attached to the temperature controller and measures the temperature of the heated surface. A National Instruments PCI-6023E Multifunctional Input/Output data acquisition board is used to gather readings from all of the T-type thermocouples and the pressure transducer. The sampling rate is every 5 s. The thermocouple and pressure transducer data are used only when the standard deviation of the specimen temperature is less than a 0.25 K and the standard deviation of pressure transducer current is less than 0.1 mA over a 1 min period. The specimen is surrounded by insulation and the entire rig, minus the flow meter, is enclosed in insulation to minimize heat loss. The total heat steady state transfer rate $\dot{Q}$ is given by [11]

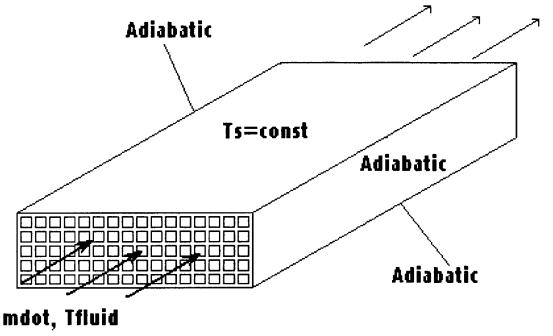

Fig. 4. Schematic of heat sink experimental configuration.

$$\dot{Q} = \dot{m} c_p \Delta T \tag{3}$$

where $\dot{m}$ is the total fluid mass flow rate (within all cells), c_p is the specific heat of the fluid, and ΔT is the temperature change from the inlet fluid temperature to the average exit fluid temperature. The fluid is allowed to mix after leaving the cells; the average as-mixed fluid exit temperature is used in calculations. The specific heat is determined from tabulated data at the mean fluid temperature. The mass flow rate is calculated using the density of air at the mean temperature of the fluid and the measured volumetric flow rate. The temperature change is determined from the measured inlet and exit temperatures. The typical inlet fluid temperature ranges from 293 K to 296 K. For the flow rates considered in this work, the mean exit fluid temperatures range from 299 K to 315 K. For all fluid velocities in this work the fluid flow in the LCA test section may be considered incompressible and laminar.

2.3. LCA heat exchanger pressure drop

The pressure drop across the LCA heat sink is of considerable interest, both to verify the laminar flow relations and to determine entrance and exit losses due to sudden inlet contraction and outlet expansion, respectively. The laminar flow pressure drop for square cells is given by [15]

$$\Delta P = fL\left(\frac{\rho_f \bar{v}^2}{2D_h}\right), \quad f = \frac{57}{Re} \tag{4}$$

$$Re = \frac{\rho_f \bar{v} D_h}{\mu}, \quad D_h = \frac{4A_c}{P_w} \tag{5}$$

Here, ΔP is the pressure drop from the inlet to exit of the LCA of length L, ρ_f is the fluid density, $\bar{v}$ is the mean velocity of the fluid in the cells, D_h is the hydraulic diameter of the flow within each cell, f is the friction factor [11], Re is the Reynolds number (based on hydraulic cell diameter), μ is the viscosity of the fluid, A_c is the cross-sectional flow area of a cell, and P_w is the wetted perimeter of this cross-sectional flow area. For the square cell with inside cell diameter d, $A_c = d^2$ and $P_w = 4d$, giving $D_h = d$.

We next compare the pressure drop from laminar flow theory augment by inlet and exit loss factors with experimental results for room temperature air (no heat-

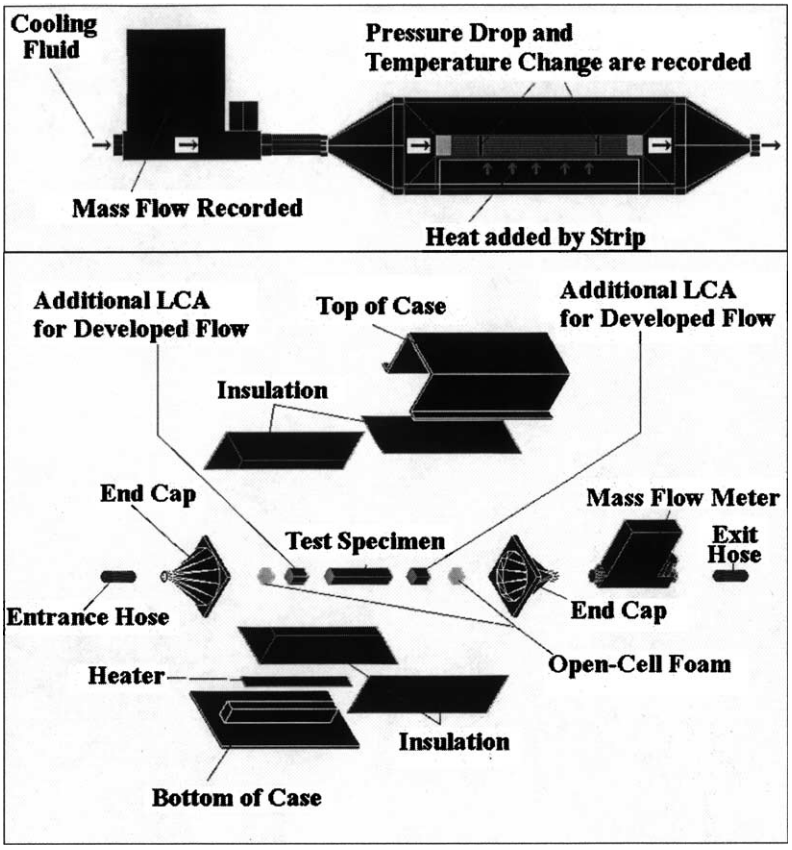

Fig. 5. Heat sink experimental configuration: (top) side-view in cross section, and (bottom) assembly view.

ing) for both steel and Cu LCA specimens with lengths ranging from 4.68 cm to 19.61 cm. The inlet and the outlet regions are shown in Fig. 6. When a fluid moves from a large orifice to a smaller one and then back to a large orifice again, head losses due to these contraction and expansion events are approximately accounted for by [16]

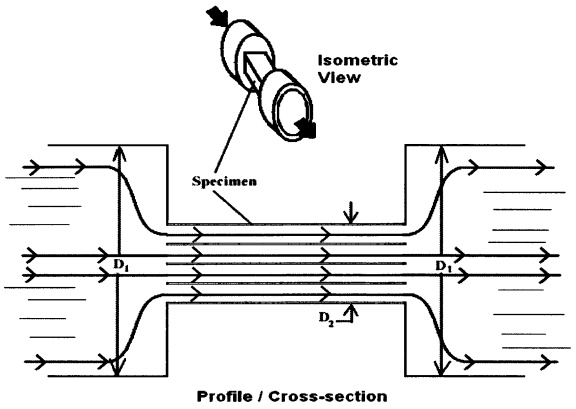

Fig. 6. Air flow through the LCA heat sink (specimen).

$$h_L = K\frac{\bar{v}^2}{2g} \tag{6}$$

where h_L is the head loss associated with each mechanism, g is the gravitational constant, and K is the loss coefficient.

According to Fig. 6, $D_1 = 4.50$ cm and each channel has a cell diameter $d = 1.35$ mm. Specimen cross sections are comprised of an 8×8 array of cells in all cases. Therefore D_2/D_1 is equal to (1.08 cm)/(4.50 cm) or 0.24. The loss coefficient, K_I, for the abrupt contraction of flow from a large diameter, D_1, to a smaller diameter, $D_2 \approx 0.24D_1$, is 0.476 [15]. The expansion loss coefficient, K_E, for the same ratio of D_1 to D_2 is equal to 0.836. Using Bernoulli's equation, the head loss is given by [15]

$$\frac{P_1}{\gamma} + \frac{\bar{v}_1^2}{2g} + z_1 = \frac{P_2}{\gamma} + \frac{\bar{v}_2^2}{2g} + z_2 + \sum h_L \tag{7}$$

where P_1 is the inlet pressure, P_2 is the outlet pressure, $\bar{v}_1$, is the mean inlet velocity, $\bar{v}_2$ is mean outlet velocity, γ is the specific weight of the fluid, z_1 and $z_2 (= z_1)$ are inlet and exit heights, and $\sum h_L$ is the total head loss. The total head loss coefficient is estimated as

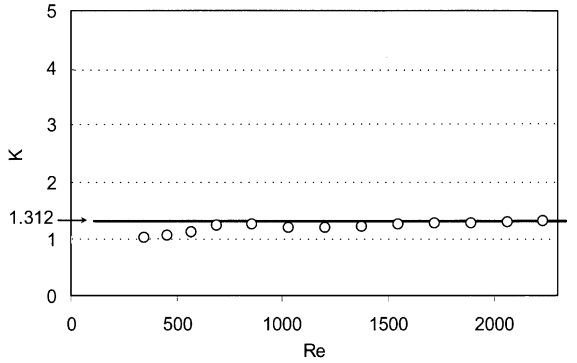

Fig. 7. Plot of head loss coefficient, K, versus Re. Inlet and outlet head losses ($K_{total} = 1.312$) compared to experimental results for 8×8 square cell array LCAs with cell size dimensions, $d = 1.35$ mm, $t = 0.10$ mm, $L = 4.68$ cm. All pressure drop measurements were recorded for room temperature airflow.

$K_{total} = K_I + K_E = 1.312$. Fig. 7 plots the head loss coefficient versus Reynolds number; K is nearly constant with respect to Reynolds number, as is expected for laminar flow. The majority of the losses are the result of sudden contraction or expansion of the flow.

2.4. Total steady state heat transfer rate

Results of steady state heat transfer rate measurements for the LCA heat sink shown in Fig. 8 pertain to a pure Cu LCA heat sink with a heated length on one side of 50.8 mm, cooled with air. The inlet fluid temperature is 293 K and the fluid flow velocity is 1.617 m/s. On the heated side, a temperature controller is used to hold the heat source at a constant temperature. The temperature difference between the center of the heater and its ends was less than 2 K. The other three sides of the LCA are insulated. The specimens all have an 8×8 array of cells in cross-section. The wall thickness, $t = 0.12$ mm, is uniform, as is the base dimension of the square cells, $d = 1.60$ mm. The external width of the specimen is 1.38 cm. At each flow rate and wall temperature level, the system was allowed to reach steady-state. Figs. 8–10 plot the measured total steady state heat transfer rate as a function of the temperature difference between the heated surface and inlet air at various Reynolds numbers. Linear regression lines are constrained to pass through zero total heat transfer rate

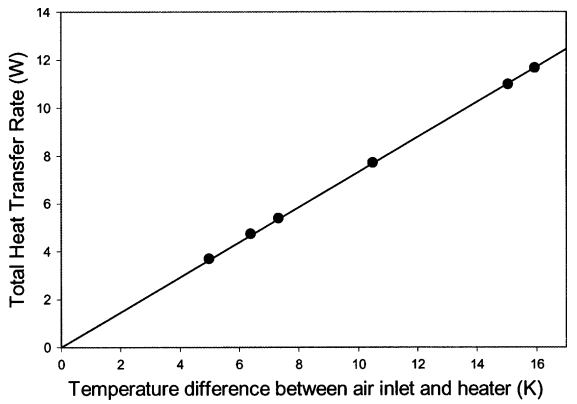

Fig. 8. Measured total heat transfer rate as a function of the temperature difference between the heater and the inlet fluid temperature for $Re = 395$. The dimensions of the Cu LCA are overall width = 1.38 cm, overall length = 5.08 cm, internal cell diameter = 1.60 mm, and wall thickness = 0.12 mm.

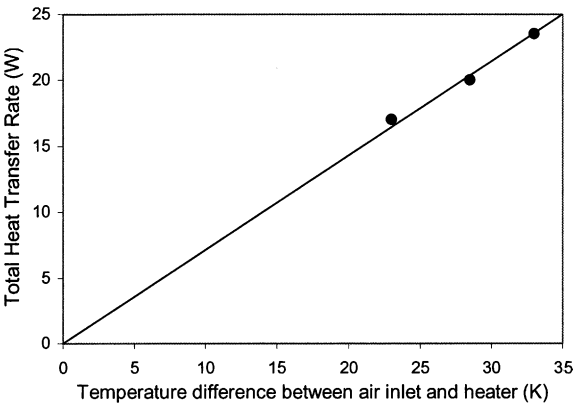

Fig. 9. Measured total heat transfer rate as a function of the temperature difference between the heater and the inlet fluid temperature for $Re = 891$. The dimensions of the Cu LCA are overall width = 1.38 cm, overall length = 5.08 cm, internal cell diameter = 1.60 mm, and wall thickness = 0.12 mm.

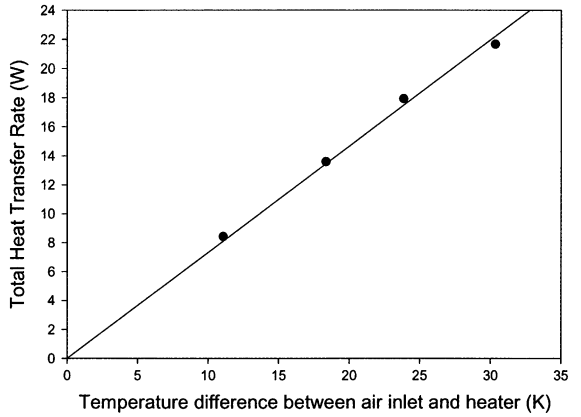

Fig. 10. Measured total heat transfer rate as a function of the temperature difference between the heater and the inlet fluid temperature for $Re = 1200$. The dimensions of the Cu LCA are overall width = 1.38 cm, overall length = 5.08 cm, internal cell diameter = 1.60 mm, and wall thickness = 0.12 mm.

when the temperature difference between the fluid at the inlet and the LCA is zero, i.e., at room temperature (293 K). The Reynolds number (Eq. (5)) is based on the cell diameter as the characteristic length. Comparison of the experimental results shown in Figs. 8–10 shows only a 1.28% variation in Nusselt number at the different Reynolds numbers. Hence, the Nusselt number is independent of Reynolds number as expected for laminar flow.

3. Comparison of experiments and simulations

A laminar flow finite difference code developed by Dempsey [17] was validated with the commercial CFD simulation code FLUENT [18] and used to predict the steady state heat transfer performance of the LCA heat sinks. The finite difference model solves the linear system of equations that result from the discretization of the three-dimensional steady state heat transfer problem. The finite difference model employs a modified successive over-relaxation (SOR) technique to solve the unsymmetric heat transfer coefficient matrix. This model discretizes the cross-section of the LCA into $2n + 1$ divisions where n is the number of flow channels or cells in the LCA. The length of the LCA is discretized into divisions of the same size as the divisions in the cross-section. This is an approximation that provides a first order solution to the steady state heat transfer problem that addresses each cell, while promoting solution efficiency. The boundary conditions are prescribed as constant temperature on one side of the LCA, with the other three sides insulated, as in experiments.

A convergence study was performed on the finite difference model to assure that the discretization was appropriate. The fluid properties are evaluated at the mean fluid temperature of the inlet and exit. The functions used to evaluate the fluid properties are curve fits to tabulated data. During the iteration scheme in the Modified SOR method, the difference between the previous value of the nodal temperature and the newly calculated temperature is set to be no greater than 10^{-6} K. In the FLUENT simulation, a convergence study was also performed on the mesh size. The mesh used in the FLUENT simulations was four times as dense as the mesh used in the finite difference. The properties used in FLUENT were also temperature dependent. However, these properties were evaluated at each nodal temperature for the fluid. The material properties of the solid were assumed constant over the temperature range explored in this work for all models.

Figs. 11 and 12 compare the predicted total heat transfer rate with the experimental results for $Re = 1200$ and $Re = 891$, respectively. The finite difference simulations agree well with the experimental results and the CFD results. The finite difference code and the CFD analyses slightly over-predict the heat transfer rate because of the minor losses that exist in the actual system. The only point that substantially differs is for the case of $Re = 891$ and temperature of approximately 311 K, likely attributed to experimental error.

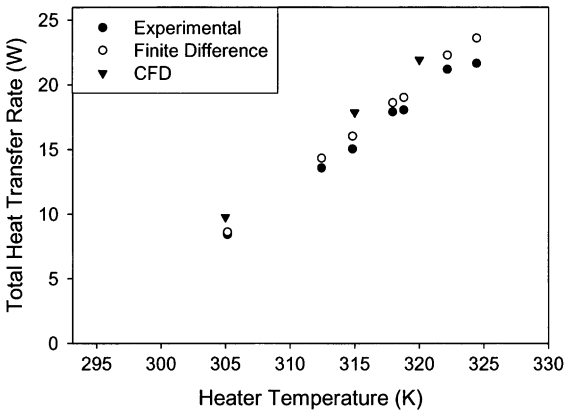

Fig. 11. Comparison of experimental results for total heat transfer rate as a function of heater temperature to finite difference predicted values for $Re = 1200$. The dimensions of the Cu LCA are overall width = 1.38 cm, overall length = 5.08 cm, internal cell diameter = 1.60 mm, and wall thickness = 0.12 mm.

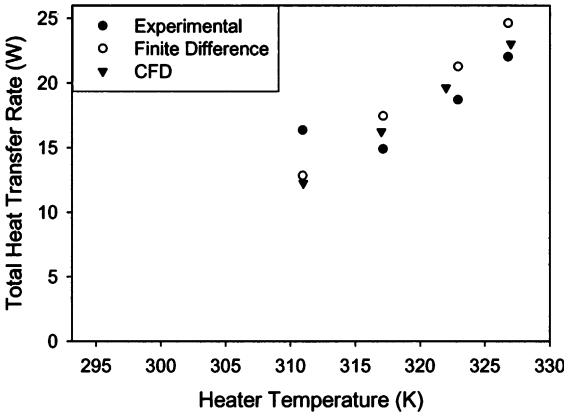

Fig. 12. Comparison of experimental results for total heat transfer rate as a function of heater temperature to finite difference predicted values for $Re = 891$. The dimensions of the Cu LCA are overall width = 1.38 cm, overall length = 5.08 cm, internal cell diameter = 1.60 mm, and wall thickness = 0.12 mm.

4. Comparison of LCA and open cell stochastic foam heat sinks

The stochastic foams studied by Bastawros and Evans [1] were subjected to a maximum pressure drop of 300 Pa for an inlet air velocity of 4 m/s. Using the

same dimensions (overall height = 20 mm, length = 25 mm, and width = 25 mm) and relative density as used in the stochastic foam experiment while maintaining laminar flow conditions, the pressure drop can be calculated for a LCA heat sink with a square cells and a base dimension of 1.60 mm and a wall thickness of 0.115 mm. These internal dimensions are selected because they fall well within the range of LCAs currently being produced, and fall approximately in the range of robust [19] or optimal [20] design sizes for forced flow convective heat transfer through LCAs. Combining Eqs. (4) and (5), and neglecting inlet and exit head losses,

$$\Delta P = \frac{57\mu\bar{v}}{2D_h^2}L \tag{8}$$

Limiting the mass flow rate per cell to 6.49×10^{-5} kg/s ensures that the flow just remains laminar ($\bar{v} = 25.6$ m/s and $Re = 1954$). A square cell LCA with these dimensions can fit 14 columns and 11 rows of cells. For the case where the height is 20 mm, the total pressure drop is 134 Pa and the total steady state heat transfer rate is 86.2 W. This translates to an equivalent flux of 107,600 W/m^2. The stated goal of Ref. [1] was to reach 10^7 W/m^2, but the reported values were two orders shy of that value. The square cell LCA heat sinks studied in this paper facilitate a heat flux on the same order of magnitude as that of the stochastic cellular metal heat sink, achieved *at less than half the pressure drop* suffered by the stochastic cellular metal heat sink due to its turbulent flow characteristics.

It is noted that with more sophisticated design approaches [19,20], it is possible to functionally grade the cell size and even cell shape to enhance the ratio of steady state heat transfer to pressure drop obtained for uniform square cell heat sinks. In addition, we may combine heat transfer requirements with additional objectives of elastic stiffness, strength, and buckling resistance of the heat sink, viewing it as a multifunctional structural member with heat transfer capabilities. Such multifunctional materials have potential applications in actively cooled aircraft skins and high temperature engines, for example, which are obvious classes of application for these extruded metallic materials under pursuit.

5. Conclusions

This paper considers the characterization of DRM LCAs for laminar flow heat sink applications. The thermal conductivity based on measured diffusivity is consistent with values expected for a material with several percent porosity [13]. This finding suggests a lack of contaminates that could adversely reduce cell wall thermal conductivity. The experimentally measured pressure drop for unidirectional fluid flow in the honeycomb channels and the total heat transfer rate of LCA heat sinks are compared to predictions from both finite difference and commercial computational fluid dynamics (CFD) codes. It is shown that flow is laminar and entry and exit head losses are well characterized.

Heat transfer performance of a stochastic cellular metal heat sink with external dimensions of height = 20 mm, length = 25 mm, and width = 25 mm [1] and an inlet velocity of 4 m/s is compared to that of a LCA heat sink of the same external dimensions and temperature boundary conditions, with top and bottom walls held fixed at 373 K. The LCA provides comparable heat removal at half the pressure drop. This ability of square cell LCAs to provide relatively high steady state heat transfer rates at relatively low pressure drop via laminar flow is attractive in electronic package cooling applications, for example. Because they are extruded with closed exterior faces, LCA heat sinks can be designed with internal bypass (selectively larger interior cells), offer low noise characteristics, and can be operated with other higher conductivity working fluids such as water at higher Biot numbers [8] to achieve enhanced heat transfer. It would be interesting to consider comparisons of relative performance of such LCA heat sinks operated at higher air flow rates in the turbulent flow regime with that of stochastic metal foam heat sinks.

Acknowledgment

This work was sponsored by DSO of DARPA (N00014-99-1-1016) under Dr. Leo Christodoulou and by ONR (N0014-99-1-0852) under Dr. Steven Fishman.

References

[1] A.-F. Bastawros, A.G. Evans, Characterization of open-cell aluminum alloy foams for high power electronic devices, in: D. Agonafer et al. (Eds.), CAE/CAD and Thermal Management Issues in Electronic Systems, ASME Conf. Proc. EEP-23/HTD-356, vol. 1, Dallas, TX, 1997, pp. 1–6.

[2] M.F. Ashby, A.G. Evans, N.A. Fleck, L.J. Gibson, J.W. Hutchinson, H.N.G. Wadley, Cellular Metals: A Design Guide, Butterworth-Heinemann, Boston, Massachusetts, 2000.

[3] M. Miscevic, L. Tadrist, R. Santini, R. Yu, Porous compact heat exchangers using metallic foams, in: Proceedings of International Conference on Compact Heat Exchangers and Enhancement Technology for the Process Industries, Banff, Alberta, Canada, 1999, pp. 191–198.

[4] T.J. Lu, H.A. Stone, M.F. Ashby, Heat transfer in open-cell cellular metals, Acta Mater. 46 (1998) 3619–3635.

[5] T.J. Lu, Heat transfer efficiency of metal honeycombs, Int. J. Heat Mass Transfer 42 (1999) 2031–2040.
[6] S. Gu, T.J. Lu, A.G. Evans, On the design of two dimensional cellular metals for combined heat dissipation and structural load capacity, Int. J. Heat Mass Transfer 44 (2001) 2163–2175.
[7] J.K. Cochran, K.J. Lee, D.L. McDowell, T. Sanders, Jr., B. Church, J. Clark, B.M. Dempsey, A. Hayes, K. Hurysz, T. McCoy, J. Nadler, R. Oh, W. Seay, B. Shapiro, Low density monolithic metal honeycombs by thermal chemical processing, in: Fourth Conference on Aerospace Materials, Processes and Environmental Technology, Huntsville, Alabama, September 18–20, 2000.
[8] A.M. Hayes, A.-J. Wang, B.M. Dempsey, D.L. McDowell, Mechanics of linear cellular alloys, Mech. Mater. 36 (8) (2004) 691–713.
[9] W.J. Parker, R.J. Jankins, C.P. Butler, G.L. Abbott, Flash method of determining thermal diffusivity, heat capacity, and thermal conductivity, J. Appl. Phys. 32 (1961) 1679–1684.
[10] S. Graham, Jr., Effective Thermal Conductivity of Damaged Composites, Ph.D. thesis, Georgia Institute of Technology, GWW School of Mechanical Engineering, Atlanta, GA, 1999.
[11] F.P. Incropera, D.P. DeWitt, Fundamentals of Heat and Mass Transfer, third ed., John Wiley & Sons, New York, 1996.
[12] J.R. Davis, ASM Specialty Handbook: Copper and Copper Alloys, ASM International, Materials Park, Ohio, 2001.
[13] B.C. Church, B.M. Dempsey, J.L. Clark, T.H. Sanders, Jr., J.K. Cochran, Copper alloys from oxide reduction for high conductivity applications, in: Proceedings of IMECE 2001, 2001 International Mechanical Engineering Congress and Exposition, New York, NY, 2001.
[14] G.F. Bocchini, The influence of porosity on the characteristics of sintered materials, The International Journal of Powder Metallurgy 22 (1986) 185–202.
[15] J.A. Roberson, C.T. Crowe, Engineering Fluid Mechanics, 6th ed., John Wiley & Sons, New York, NY, 1997.
[16] I. Granet, Fluid Mechanics, 4th ed., Prentice Hall, Englewood Cliffs, NJ, 1996.
[17] B.M. Dempsey, Thermal Properties of Linear Cellular Alloys, M.S. thesis, Georgia Institute of Technology, GWW School of Mechanical Engineering, Atlanta, GA, 2002.
[18] FLUENT User's Guide, Release 6.0.20. FLUENT Inc., 1998.
[19] C.-C. Seepersad, B.M. Dempsey, J.K. Allen, F. Mistree, D.L. McDowell, Design of multifunctional honeycomb materials, AIAA J. 42 (5) (2004) 1025–1033.
[20] R.S. Kumar, D.L. McDowell, Rapid preliminary design of rectangular linear cellular alloys for maximum heat transfer, AIAA J. 42 (8) (2004) 1652–1661.